Progress In Electromagnetics Research Letters, Vol. 92, 85–92, 2020

Single-Substrate Double-Side High Selectivity Frequency Selective Surface

Xiaofan Yang[1], Liandong Wang[1], Xujian Shen[1], Xiaoming Liu[2, 3, *], Tao Qi[2], and Yixin Zhou[2]

Abstract—Frequency selective surface is a key component in applications such as communication antenna and remote sensing radiometer. One of the core parameters is selectivity, which is usually realized using a multi-layer structure or through a complicated 3D structure. These methods, however, would impose much challenge on alignment or fabrication. This paper proposes a single-substrate and combined-united array to realize a high selectivity frequency selective surface. The unit cell is a combined pattern of cross dipole and square loop to generate double transmission zeroes out of the passband. Both sides of the substrate are printed with the same pattern to enhance the selectivity. Such a structure enables easy fabrication and assembly by avoiding using multi-substrates. A prototype in the Ku-band demonstrates that both sides of the passband show high selectivity.

1. INTRODUCTION

Frequency selective surface (FSS) is a type of signal conditioning component acting as a spatial filter and has seen a wide range of applications such as communication antenna [1], frequency separation in a quasi-optical system [2], and dual-frequency output in a high-power gyrotron system [3]. To accommodate different applications, the specifications of an FSS varies accordingly. In a remote sensing radiometer, high selectivity is required to separate two adjacent bands. A typical case is the need of separation of 89 GHz and 118 GHz [4], where the transition region is very narrow.

A high-selectivity FSS normally has very narrow transition region between passband and rejection band. Many techniques have been developed to design high-selectivity FSS, such as multi-layer structure [5, 6], multi-element structure [7, 8], antenna-filter-antenna (AFA) structure [9, 10], substrate integrated waveguide (SIW) structure [11, 12], and 3D structure [13, 14]. Also, FSSs can be made of all-dielectric materials [15], printed surfaces [16], and all metal structures [17]. Multi-layer structure is the most commonly used technique for high-selectivity FSS design. Though cascading identical layers gives one good edge roll off, fabrication and alignment difficulties are its by-products. A multi-element structure is usually used to create multi-band operation, which may not be always necessary. AFA structure is a three-layer structure with the top and bottom layers patterned with antenna array and the middle layer with coupling slots. Such a structure creates transmission zeros at the edge of the passband so that a quasi-elliptical response can be realized. Unfortunately, the top and bottom layers have to be printed on two different substrates, and the middle layer has to be sandwiched into the two substrates with very low tolerance of air gap. This difficulty has already been manifested in [18]. SIW technique has been rapidly developed in recent years. Many good properties have been observed. When it is used as high-selectivity FSS, up to six layers may be used, making the components too thick to

Received 11 April 2020, Accepted 12 June 2020, Scheduled 29 June 2020

* Corresponding author: Xiaoming Liu (xiaoming.liu@ahnu.edu.cn).

[1] State Key Laboratory of Complex Electromagnetic Environment Effects on Electronics and Information System, Luoyang 471003, China. [2] School of Physics and Electronic Information, Anhui Normal University, Wuhu, Anhui 241002, China. [3] Anhui Provincial Engineering Laboratory on Information Fusion and Control of Intelligent Robot, Wuhu, Anhui 241002, China.

use in real applications. 3D structure has the advantage of generating more transmission poles and zeros, making its tunability even better than a planar 2D structure. The complexity in a 3D structure, however, may impose much more challenge on fabrication when it goes to very high frequency. Recently, artificial intelligence-based approaches, such as Ant Colony [19] and Neural Networks [20, 21], have been used to design FSSs as well as other electromagnetics components. These methods may also be helpful for design of high-selectivity FSS.

To maintain good selectivity while not introducing too much fabrication difficulty, the capacity of 2D structure is still worth of investigation. In [22], a combined unit cell has been investigated to create elliptical response so that high-selectivity can be achieved. Combining two different patterns to a unit cell gives one more freedom to control the positions of transmission poles and zeros. This structure, unfortunately, is again a multi-substrate structure separated by air gap. Such a structure is not suitable for radiometers deployed on an airborne platform. To enhance mechanical stability, the two layers have to be printed on a single substrate. Actually, due to their low cost and ease of fabrication, single-substrates can also be used as partially reflecting surfaces with aperture antenna to drastically improve their radiation patterns and antennas performance [23], or used for reconfiguring antennas [24].

This work presents a class of FSS using a single substrate and combined unit cell to realize double-side high-selectivity response. Single substrate provides one with easy fabrication and installation to a real system, without compromising the performance significantly. This is one novelty of this design. In addition, single substrate avoids a too thick design. Combined unit cell is capable of creating high-selectivity response, which is the second novelty of this work.

The remaining of this paper is organized as follows. Section 2 describes the design procedures. Section 3 is devoted to fabrication and measurement. Section 4 concludes this work.

2. DESIGN AND OPTIMIZATION

Cross dipole and square loop unit cells are usually used in the design of an FSS. To increase bandwidth and selectivity, a multi-layer structure may be used, as shown in Figures 1(a) and (b). However, such a structure limits selectivity because the transmission zeros are too far from the transmission poles. In this connection, a combined design has been proposed as shown in Figure 1(c). Such a design consists

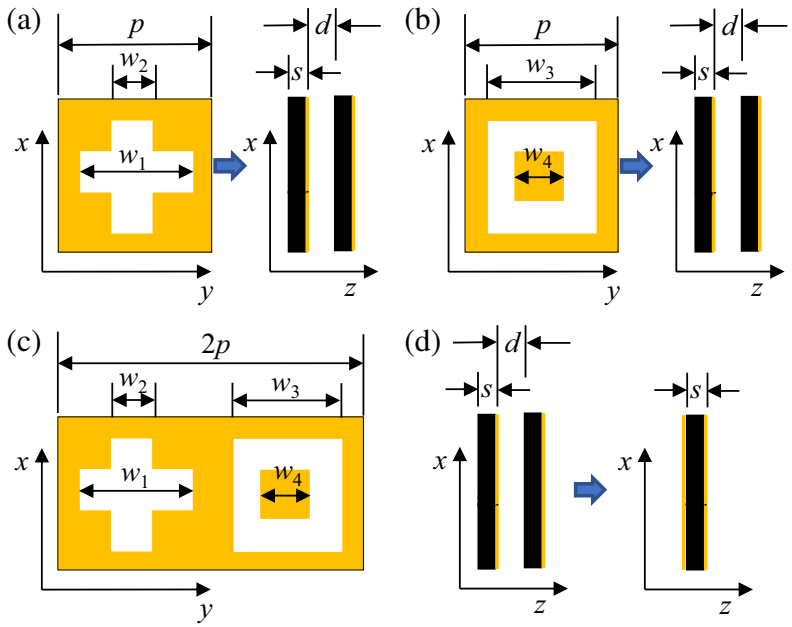

Figure 1. Development of single-substrate FSS of high selectivity. (a) Cross type of two substrates; (b) loop type of two substrates; (c) combined type with cross dipole and loop unit cell; (d) from two substrates to single substrate.

of a cross dipole and a square loop. Improved bandwidth and selectivity can be obviously observed [22].

However, this improvement is yet satisfactory. Since two substrates are used, the assembly of such an FSS to a real quasi-optical system requires a spacer between the two substrates. In many applications, the FSS is used in a high-vibration environment. Therefore, a single layer substrate is superior to the design of Figure 1(c). In light of this, the design of Figure 1(d) is proposed. The proposed design has only one substrate, and both sides are printed with the combined pattern, forming an array-substrate-array structure.

To reveal the evolution of the design, four cases are simulated as shown in Figure 2. The first case is a two-layer cross dipole patterned on a single substrate, see Figure 2(a). The unit cell is half the length of the final design. An LTCC substrate is used. The dielectric constant is 3.9. It is seen that a transmission pole takes place at 14.09 GHz, and a transmission zero is observed at 12.93 GHz. However, there is no transmission pole on the high frequency side. For the second case shown in Figure 2(b), the transmission pole is located at 15.17 GHz, and the transmission zero is 16.63 GHz. Unfortunately, the bandwidth is not sufficiently good. For the cases of Figure 2(c) and Figure 2(d), the unit cell is the same as the final design. It is seen that, both cases see slight shift of transmission poles and zeros. However, the frequency shift does not change the response curve significantly. It can be concluded that by only using a cross dipole or square loop, the selectivity will not be enhanced noticeably, or the bandwidth is not good enough.

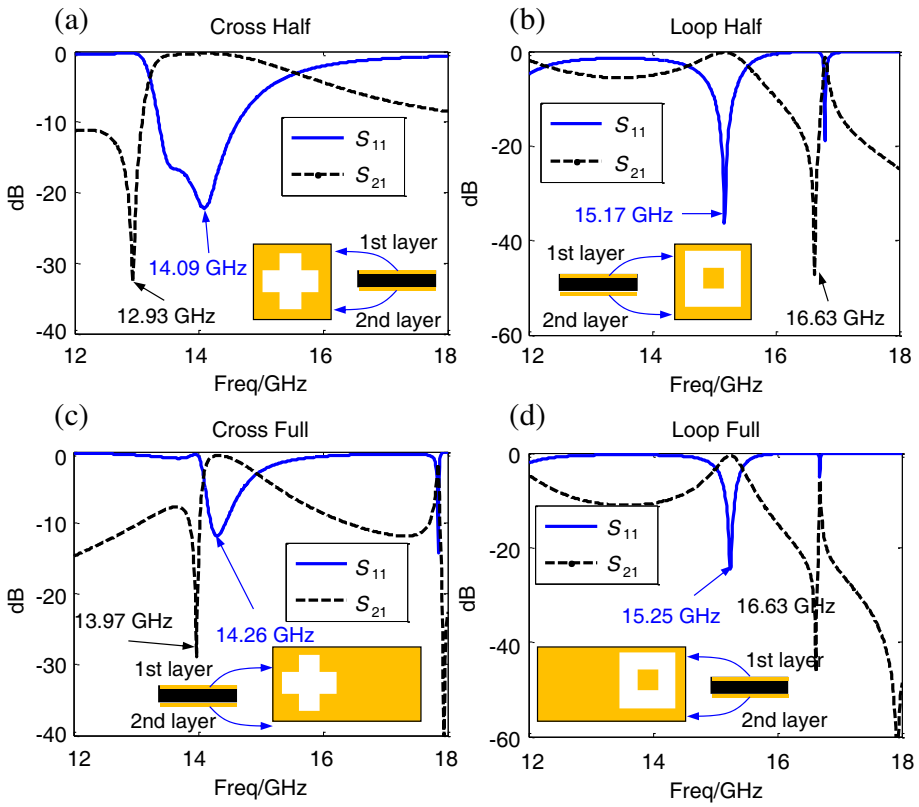

Figure 2. Simulation results of (a) two-layer single-substrate cross dipole of half-length unit cell; (b) two-layer single-substrate square loop of half-length unit cell; (a) two-layer single-substrate cross dipole of full-length unit cell; (b) two-layer single-substrate square loop of full-length unit cell.

Combine the cross dipole and square loop to form a new unit cell. Through careful optimization, a satisfactory design is obtained. The optimized parameters are tabulated in Table 1, and the simulation results are plotted in Figure 3. It is clearly shown that the transmission poles are located at 14.26 GHz and 15.10 GHz. The former is due to the cross dipole, and the latter is produced by the square loop. The first transmission zero takes place at 13.75 GHz, which is from the cross dipole. The transmission

Table 1. Parameters for Figure 1 and Figure 2, unit is mm.

Parameters	Value
p	9.3 mm
w_1	7.6 mm
w_2	1.9 mm
w_3	5.3 mm
w_4	4.5 mm
d	1.5 mm
s	1.5 mm
ε_r	3.9

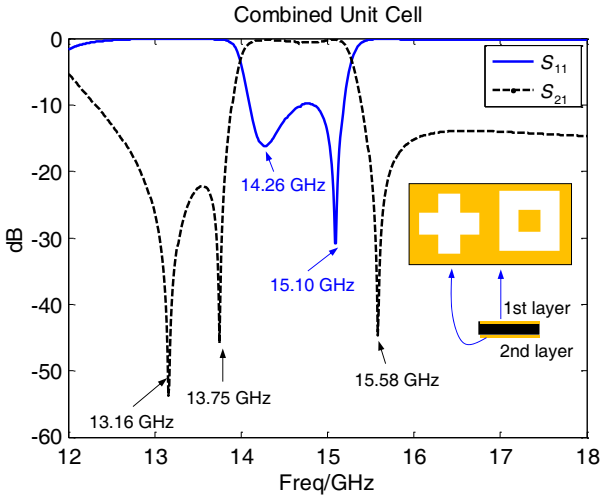

Figure 3. Simulation results of two-layer single-substrate combined structure of cross dipole and square loop.

zero at 15.58 GHz is from the square loop. Compared to the results of Figure 2(c) and Figure 2(d), it is noted that combination of the cross dipole and square loop does not affect the transmission pole too much. However, the transmission zero around 16 GHz is redshifted to 15.58 GHz. In addition, a new transmission zero emerges at 13.16 GHz. However, these changes give one a better design, generating much higher selectivity as well as providing better bandwidth. Such an observation gives a design guideline that one needs to choose the transmission poles properly so that a combined unit cell would lead to a satisfactory design.

In addition, it can be deduced that the -3 dB bandwidth is 1.27 GHz (14.0–15.27 GHz), and the -20 dB bandwidth is 1.69 GHz (13.81–15.50 GHz). Therefore, the rectangular coefficient of the passband is $\mathrm{BW}_{3\,\mathrm{dB}}/\mathrm{BW}_{20\,\mathrm{dB}} = 0.752$.

To shed some light on the design, the equivalent circuit model is shown in Figure 4. The cross dipole can be modelled using a parallel circuit [25], and the square loop can be represented using a series resonator [26] in conjunction with a shunt inductor. A slot can be modelled as a capacitor, and the metallic strip can be modelled as an inductor. Patch can also be modelled as an inductor. In this regard, the slot array is equivalent to a parallel circuit, and the square loop is equivalent to a series resonator in shunt with a parallel inductor L'. The combined unit cell can be modelled using the shut circuit of each equivalent model. The substrate can be represented using a transmission line, with the admittance of Y_d and electrical length of θ_d. These factors all together create the response results shown in Figure 4. However as it is mentioned, to arrive at a proper design, the transmission poles are most

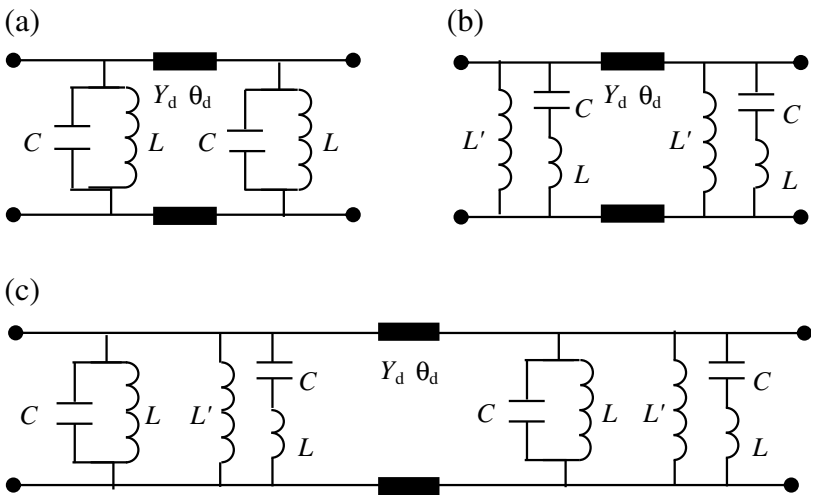

Figure 4. Equivalent circuits for (a) cross dipole, (b) square loop, and (c) the combined unit cell.

important. They have to be close to each other to form a passband. And the transmission pole of square loop has to be higher than that of the cross dipole so that both sides of the passband have high selectivity.

3. FABRICATION AND MEASUREMENT

The substrate is LTCC produced by NEC Corporation. The provided dielectric constant is 3.9. A free-space measurement gives $3.88 \times (1 - j0.003)$ in the range of 12–18 GHz [27], which is very close to the provided value. The fabricated FSS is shown in Figure 5(a), and the dimension of the FSS is 12 cm by 12 cm.

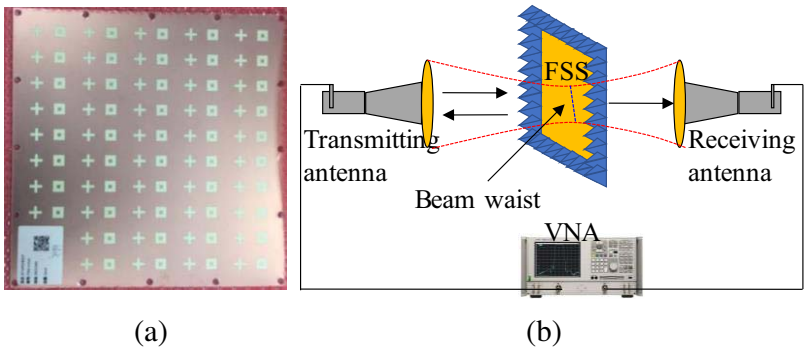

Figure 5. Fabricated FSS and measurement. (a) Photography; (b) measurement setup.

The measurement is conducted using a spot-focusing antenna system. A lens is mounted on the aperture of the transmitting/receiving antenna, creating a focused spot at the location of the FSS. The diameter of the spot is smaller than the width of the fabricated FSS. The transmitting and receiving antennas are connected to a vector network analyzer (Ceyear AV3276D). The VNA is calibrated using the traditional SLOT method. An open through of air is then measured, serving as the background measurement. Time gating technique is applied so as to remove residual multi-reflection. Lastly, the FSS is placed on a sample holder for measurement.

The measured results are plotted in Figure 6 in comparison with the simulated ones. It is clearly demonstrated that the measured results are overall in good agreement with the simulated ones. The in-band insertion loss is around 0.8 dB, slightly higher than the simulated 0.6 dB. The simulated curves

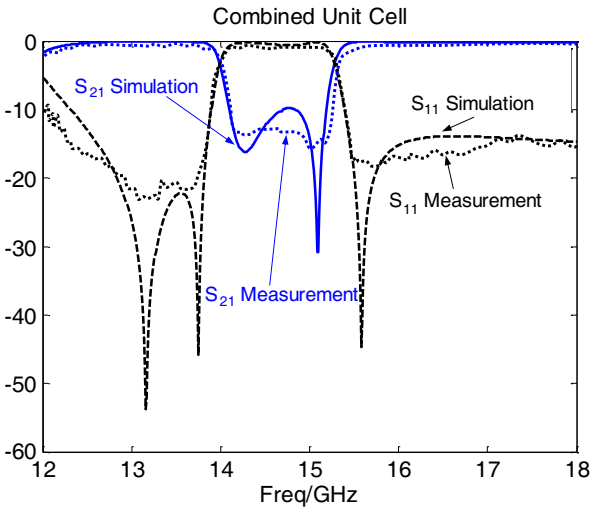

Figure 6. Comparison of simulation and measurement.

Table 2. A comparison of the bandpass FSS using different number of substrate layer.

Reference	Number of layers	Selectivity
[5]	8	0.6
[6]	3	0.5
[9]	2	< 0.6
[10]	4	0.5
[13]	2	< 0.5
[14]	2	< 0.5
[28]	2	< 0.25
This work	1	0.752

exhibit very obvious transmission zeros. In comparison, the measured results do not show very sharp nulls. This is probably due to the cutting effect of the time gating technique or the residual noise.

A comparison of this work with other multi-layer structures is presented in Table 2. It is seen that with the increase of layer number, the selectivity does see improvement. However, this work demonstrates better selectivity ($BW_{3\,dB}/BW_{20\,dB} = 0.752$). Such a result clearly show that this design is effective to enhance the selectivity. This improvement may be attributed to the use of combined unit cells.

However, this structure also has its limitation. The most obvious limitation is the bandwidth. To form a bandpass FSS using this structure, the transmission pole of each unit cell has to be close to each other. This requirement makes the passband not so easily tunable. It is more suitable for narrowband applications.

4. CONCLUSION

A double-side high selectivity frequency selective surface has been designed, fabricated, and measured. This design uses a combined unit cell of cross dipole and square loop. These unit cells are printed on both sides of an LTCC substrate. Such a design forms a dual-layer structure. The combination creates multiple transmission zeros and poles. In comparison to the cross-dipole array, a better selectivity is formed. Compared to a square-loop array, a better bandwidth is found. Particularly, both sides of the passband have good selectivity. This design will ease the fabrication and assembly. Future efforts may be focused on increasing the bandwidth or using more combined units to increase the selectivity.

ACKNOWLEDGMENT

This work is supported by the Open Project of the State Key Laboratory of Complex Electromagnetic Environment Effects on Electronics and Information System under the number of CEMEE2020Z0205A, and the National Natural Science Foundation of China under the contract numbers of 61871003.

REFERENCES

1. Li, Y., P. Ren, and Z. Xiang, "A dual-passband frequency selective surface for 5G communication," *IEEE Antennas and Wireless Propagation Letters*, Vol. 18, 2597–2601, 2019.
2. Liu, X., Y. Wang, T. Zhang, et al., "A compact multi-band quasi-optical system for plasma detection," *IEEE Transactions on Antennas and Propagation*, Vol. 68, 4916–4924, 2020.
3. Li, X., X. Liu, K. Ronald, et al., "Investigation of frequency-selective surfaces for a THz gyromultiplier output system," *IEEE Transactions on Electron Devices*, Vol. 64, 4678–4685, 2017.
4. Lawrence, H., N. Bormann, A. J. Geer, et al., "Evaluation and assimilation of the microwave sounder MWHS-2 onboard FY-3C in the ECMWF numerical weather prediction system," *IEEE Transactions on Geoscience and Remote Sensing*, Vol. 56, 3333–3349, 2017.
5. Shen, Y., D. Chen, Q. Wei, et al., "183-GHz frequency selective surface using aligned eight-layer microstructure," *IEEE Transactions on Electron Devices*, Vol. 39, 1612–1615, 2018.
6. Tao, K., B. Li, Y. Tang, et al., "Multi-layer tri-band frequency selective surface using stepped- and uniform-impedance resonators," *Electronics Letters*, Vol. 52, 583–585, 2016.
7. Yu, Z., X. Yang, J. Zhu, et al., "Dual-band three-dimensional FSS with high selectivity and small band ratio," *Electronics Letters*, Vol. 55, 798–799, 2019.
8. Lü, M., M. Huang, and Z. Wu, "Design of multi-band frequency selective surfaces using multi-periodicity combined elements," *Journal of Systems Engineering and Electronics*, Vol. 20, 675–680, 2009.
9. Naseri, P., F. Khosravi, P. Mousavi, et al., "Antenna-filter-antenna-based transmit-array for circular polarization application," *IEEE Antennas and Wireless Propagation Letters*, Vol. 16, 1389–1392, 2017.
10. Li, Y., L. Li, Y. Zhang, et al., "Design and synthesis of multilayer frequency selective surface based on antenna-filter-antenna using Minkowski fractal structures," *IEEE Transactions on Antennas and Propagation*, Vol. 63, 133–141, 2020.
11. Mollaei, M. S. M., "Narrowband configurable polarization rotator using frequency selective surface based on circular substrate-integrated waveguide cavity," *IEEE Antennas and Wireless Propagation Letters*, Vol. 16, 1923–1926, 2017.
12. Varikuntla, K. K. and R. Singaravelu, "Ultrathin design and implementation of planar and conformal polarisation rotating frequency selective surface based on SIW technology," *IET Microwaves, Antennas & Propagation*, Vol. 12, 1939–1947, 2018.
13. Zhu, J., Z. Hao, C. Wang, et al., "Dual-band 3-D frequency selective surface with multiple transmission zeros," *IEEE Antennas and Wireless Propagation Letters*, Vol. 18, 596–600, 2019.
14. Lee, I. G. and I. P. Hong, "3D frequency selective surface for stable angle of incidence," *Electronics Letters*, Vol. 50, 423–424, 2014.
15. Afzal, M. U., A. Lalbakhsh, and K. P. Esselle, "Electromagnetic-wave beam-scanning antenna using near-field rotatable graded-dielectric plates," *Journal of Applied Physics*, Vol. 124, paper ID:234901, 2018.
16. Lalbakhsh, A., M. U. Afzal, and K. P. Esselle, "Multiobjective particle swarm optimization to design a time-delay equalizer metasurface for an electromagnetic band-gap resonator antenna," *IEEE Antennas and Wireless Propagation Letters*, Vol. 16, 912–915, 2017.
17. Lalbakhsh, A., M. U. Afzal, K. P. Esselle, et al., "Low-cost non-uniform metallic lattice for rectifying aperture near-field of electromagnetic bandgap resonator antennas," *IEEE Transactions on Antennas and Propagation*, Vol. 68, 3328–3335, 2020.

18. Abbaspour-Tamijani, A., K. Sarabandi, and G. M. Rebeiz, "Antenna-filter-antenna arrays as a class of bandpass frequency-selective surfaces," *IEEE Transactions on Microwave Theory and Technology*, Vol. 52, 1781–1789, 2004.
19. Lalbakhsh, P., B. Zaeri, and A. Lalbakhsh, "An improved model of ant colony optimization using a novel pheromone update strategy," *IEICE Transactions on Information and Systems*, Vol. 96, 2309–2318, 2013.
20. Jamshidi, M. B., A. Lalbakhsh, S. Lotfi, et al., "A neuro-based approach to designing a Wilkinson power divider," *International Journal of RF and Microwave Computer-Aided Engineering*, Vol. 30, 1–10, 2020.
21. Jamshidi, M. B., A. Lalbakhsh, B. Mohamadzade, et al., "A novel neural-based approach for design of microstrip filters," *AEU-International Journal of Electronics and Communications*, Vol. 110, 152847, 2019.
22. Tang, C., X. Liu, H. Wang, et al., "Design and research of highly selective frequency selective surfaces," *Proceeding of the Sixth Asia-Pacific Conference on Antennas and Propagation (APCAP)*, Xi'an, China, Oct. 16–19, 2017.
23. Lalbakhsh, A., M. U. Afzal, K. P. Esselle, et al., "Single-dielectric wideband partially reflecting surface with variable reflection components for realization of a compact high-gain resonant cavity antenna," *IEEE Transactions on Antennas and Propagation*, Vol. 67, 1916–1921, 2019.
24. Das, P., K. Mandal, and A. Lalbakhsh, "Single-layer polarization-insensitive frequency selective surface for beam reconfigurability of monopole antennas," *Journal of Electromagnetic Waves and Applications*, Vol. 34, 86–102, 2020.
25. Munk, B. A., *Frequency Selective Surfaces: Theory and Design*, Wiley, New York, 2000.
26. Liu, X., Z. Li, C. Tang, et al., "Double-square and gridded-square loop frequency-selective surface in the K-band," *Microwave and Optical Technology Letters*, Vol. 60, 1136–1142, 2018.
27. Liu, X. and J. Yu, "Characterization of the dielectric properties of water and methanol in the D-band using a quasi-optical spectroscopy," *Scientific Reports*, Vol. 9, paper ID:18962, 2019.
28. Lalbakhsh, A., U. A. Muhammad, P. E. Karu, et al., "Multi-objective particle swarm optimization for the realization of a low profile bandpass frequency selective surface," *2015 International Symposium on Antennas and Propagation (ISAP)*, Hobart, TAS, Australia, Nov. 9–12, 2017.